Available online at www.sciencedirect.com
SCIENCE DIRECT®
Earth and Planetary Science Letters 223 (2004) 1–16
EPSL Frontiers
www.elsevier.com/locate/epsl

Frontiers

The chemistry of subduction-zone fluids

Craig E. Manning*

Department of Earth and Space Sciences, University of California at Los Angeles, Los Angeles, CA 90095-1567, USA

Received 24 April 2004; accepted 27 April 2004

Abstract

Subduction zones generate voluminous magma and mediate global element cycling. Fluids are essential to this activity, yet their behavior is perhaps the most poorly understood aspect of the subduction process. Though many volatile components are subducted, H_2O is the most abundant, is preferentially fractionated into the fluid phase, and, among terrestrial volatiles, is by far the most effective solvent. H_2O therefore controls the chemical properties of subduction-zone fluids. Rising pressure (P) and temperature (T) along subduction paths yield increased H_2O ionization, which enhances dissolved solute concentrations. Under appropriate conditions, silicate solubilities may become so high that there is complete miscibility between hydrous melts and dilute aqueous solutions. Miscible fluids of intermediate composition (e.g., 50% silicate, 50% H_2O) are commonly invoked as material-transport agents in subduction zones; however, phase relations pose problems for their existence over significant length scales in the mantle. Nevertheless, this behavior provides a key clue pointing to the importance of polymerization of alkali aluminosilicate components in deep fluids. Aqueous aluminosilicate polymers may enhance solubility of important elements even in H_2O-rich fluids. Subduction-zone fluids may be surprisingly dilute, having only two to three times the total dissolved solids (TDS) of seawater. Silica and alkalis are the dominant solutes, with significant Al and Ca and low Mg and Fe, consistent with a role for aqueous aluminosilicate polymers. Trace-element patterns of fluids carrying only dissolved silicate components are similar to those of primitive island-arc basalts, implying that reactive flow of H_2O-rich, Cl-poor, alkali-aluminosilicate-bearing fluid is fundamental to element transport in the mantle wedge. Better understanding of the interaction of this fluid with the mantle wedge requires quantitative reaction-flow modeling, but further studies are required to achieve this goal.

Keywords: subduction zones; subduction-zone fluids; mantle wedge; metasomatism

1. Introduction

The segments of subduction zones extending from trenches to beneath volcanic arcs are sites of profound chemical change. Incoming lithosphere is stripped of elements [1–4] which are transferred to the overlying mantle [5–9] in a process that ultimately generates volcanic arcs. The chemical work done in this "subduction factory" is fundamental to the Earth's evolution, because it leads to prolific volcanism and degassing, it mediates the global cycling of elements, and over time it produced the continental crust.

The transfer of material in subduction zones occurs in steps, and the agents of transfer vary. It is generally thought that H_2O-rich fluid (Table 1) is initially

* Tel.: +1-310-206-3290; fax: +1-310-825-2779.
E-mail address: manning@ess.ucla.edu (C.E. Manning).

0012-821X/$ - see front matter © 2004 Elsevier B.V. All rights reserved.
doi:10.1016/j.epsl.2004.04.030

Table 1
Glossary of terms

Compatible element	An element that is preferentially partitioned into the solid in a solid–fluid mixture
Critical end point	Point defined by the intersection of a critical curve and a solubility curve
Critical curve	Curve linking critical points of end members in a two-component system. It is the boundary between stability fields of a supercritical fluid and a two phase mixture of liquid + vapor
Critical point	The termination of the liquid + vapor field in a one component system
Fluid	A disordered, non-crystalline phase consisting of particles in motion and possessing unspecified composition
Incompatible element	An element that is preferentially partitioned into the fluid in a solid–fluid mixture
Liquid	High-density, subcritical fluid
Metasomatism	The process by which rock is compositionally modified
Miscibility	The property enabling discrete phases to mix completely to form a single phase
Polymerization	In the context of this paper, the linking of cations by shared (bridging) oxygens
Solubility curve	In a simple two component system, a curve linking the eutectic with the triple point of an end member. In the system A-H_2O, the high-T solubility curve is the line along which solid A may coexist with liquid and vapor
Solidus	Reaction boundary denoting the first appearance of melt with increasing T in a multicomponent system
Supercritical	State of a system in which a single fluid phase is stable
Supercritical fluid	A fluid stable at P and T greater than the critical point or curve in the system of interest
Total dissolved solids	The sum of masses of all dissolved solutes, in g/kg H_2O
Vapor	Low-density, subcritical fluid. Synonymous with "gas"

responsible for leaching elements from the slab [8,10–13]. The fluid is liberated by metamorphic devolatilization in subducting lithosphere and carries solutes as it migrates into the overlying wedge of mantle, resulting in chemical modification, or "metasomatism," of slab and wedge. As the process continues, the fluid triggers melting, yielding voluminous magma that is chiefly basaltic in composition. These magmas serve as the second agents of mass transfer, bringing slab- and mantle-derived components toward the surface as they rise.

Although melting in subduction-zone settings can be quite complex [8,9,12,14], study of the sources and evolution of the magmas is well advanced. In contrast, we know little about the fluid that begins the process of material transfer in subduction zones. In general, understanding the compositional evolution of a moving fluid and its host rocks requires techniques that couple fluid flow with chemical reaction. Reactive flow characterizes many terrestrial environments—e.g., ore deposits, crustal metamorphic systems, sedimentary basins, mid-ocean ridges— and modeling element transport in such systems has met with success. The same cannot be said of subduction zones, primarily because we lack basic information on fluid composition and how it is controlled. No direct, pristine fluid sample can be collected from this environment and working backwards from evolved magmatic products yields insight into only a part of the flow system. In addition, experimental study of fluids at the requisite high pressure (P) and temperature (T) has proven to be a singular challenge. As a result, fundamental questions remain: are the fluids dilute solutions or silicate-rich mixtures intermediate between H_2O and melt? What is the role of ligands such as Cl? How does mineral solubility and element partitioning change along the flow path? Answering these questions requires a better understanding of the chemical behavior of the fluid phase at great depth.

In this paper, I highlight recent advances that offer preliminary insights into the chemical behavior of subduction-zone fluids. I first review the physical controls that operate along the paths of fluid flow. This is followed by discussion of the chemical properties of solutions at high P, which gives context to a summary of constraints on composition. The new results are an initial step toward a chemical foundation for investigating one of Earth's most important fluids.

2. Physical controls on subduction-zone fluids

As summarized in Fig. 1, rising P and T during subduction drive mineral reactions that yield a discrete fluid phase. The fluid is probably rich in H_2O relative to other volatiles (e.g., CO_2) because of greater abundance, favorable partitioning and low thermal

stability of hydrated silicates [15–20]. Experiments, simulations, and isotope geochemistry indicate that volatile liberation from subducted lithologies is more or less continuous [13,21–28], although instances of episodic fluid production may be indicated by slab seismicity [18,29].

The slab's capacity to produce fluid diminishes with depth, as minerals progressively transform to less volatile-rich assemblages (Fig. 1a). Although much of the slab H_2O is lost, a fraction is retained and recycled into the deep Earth in residual phases [13,30–37]. The liberated fluid is buoyant, and upon formation begins ascending toward the surface. Some fluid may move upward within the slab [38], but most evidently migrates into the overlying mantle wedge (Fig. 1a).

Movement into the mantle wedge is an important step for subduction-zone fluids. Not only is there a sudden shift in host-rock composition, but in addition mantle minerals are strongly undersaturated in volatiles. At equilibrium, free H_2O cannot exist in the mantle until formation of a fully hydrated mineral assemblage (serpentine, chlorite, talc, and amphibole) or hydrous mineral stability is exceeded. Fig. 1b illustrates that near the slab, the mantle H_2O content can increase to >5 wt.%, but this changes with position. The consumption of fluid by the mantle begins at the shallowest levels in the forearc [18,39,40], and continues to at least sub-arc depths. During subduction, the slab and overlying mantle become mechanically coupled, causing mantle material to be dragged downward (Fig. 1). This provides a mechanism to continually supply fresh, volatile-poor mantle for the uptake of fluid. Despite the efficiency of this process, some slab-derived fluid may travel great distances before being consumed, and locally may even reach the surface (Fig. 1a). A natural example of the surficial venting of slab-derived fluids may occur at Kinki, Japan [41].

The down-going mantle cuts across mineral stability boundaries, causing volatile-bearing minerals to regenerate the fluid they earlier absorbed (Fig. 1b). Several such events may occur, until stable minerals become nominally anhydrous. From this point on, the mantle can no longer consume the fluid phase, leaving it free to flow upwards to trigger arc-magma production. Hence, a given fluid "particle" in subduction zones experiences a stepwise history, with discrete flow events interspersed between periods of movement while dissolved in solids.

Subduction-zone fluids migrate along paths of increasing temperature with decreasing pressure (Fig. 1c). The fluid path illustrated in Fig. 1 involves a T increase from $\sim$ 500 °C at 100-km depth ($\sim$ 3.2 GPa), to $\sim$ 1150 °C, at 80-km depth ($\sim$ 2.4 GPa). The increase of 650 °C over $\sim$ 20 km (32.5 °C/km) probably represents a maximum gradient because the model system on which the figure is based represents an old, cold subduction system [42]. Nevertheless, increasing T during decompression is unusual among terrestrial fluid-flow systems, and it has important consequences for chemical behavior.

Fluid flow in the mantle wedge may involve porous flow, channeled flow, or a combination [20,43–45]. During porous flow, fluids intimately interact with the rock matrix, leading to a strong potential for continuous equilibration with the host material along the flow path, such that the rock matrix controls the composition of the fluid. By contrast, channelized flow produces zones in which the fluid-to-rock ratio is much higher. The fluid interacts with less rock per unit volume and retains more of its initial source composition. Porous and channelized flow will have significantly different velocities of several m/year vs. hundreds of m/year, respectively. U–Th–Ra disequilibria in arc magmas [46,47] and distances implied by Fig. 1 suggest 2.5 to $\sim$ 100 m/year, which is consistent with both channelized and porous flow. It is quite possible that the velocity variations are real, reflecting a spectrum of hydrologic settings.

3. Chemical controls on the composition of subduction-zone fluids

The key step in identifying the chemical controls on fluid composition in the slab and mantle wedge is the direct measurement of mineral solubility at subduction-zone P and T. Recent advances have provided the first systematic observations of this kind [48–57]. Results demonstrate large solubility increases with increasing pressure. What governs this behavior? Important factors include the properties of solvent H_2O, the association/dissociation behavior of dissolved solutes, ligand concentrations, and the extent of formation of dense, solute-rich fluids that are intermediate between melts and H_2O.

3.1. H_2O at subduction-zone conditions

Because of its volumetric dominance, H_2O controls the properties of subduction-zone fluids. Water's polar character and greater tendency to dissociate make it a substantially more powerful solvent than other volatiles. The solvent properties of H_2O depend on the density, ordering, hydrogen bonding, and dissociation of H_2O molecules. H_2O density is 1.2–1.4 g/cm^3 at sub-arc depths (Fig. 1)

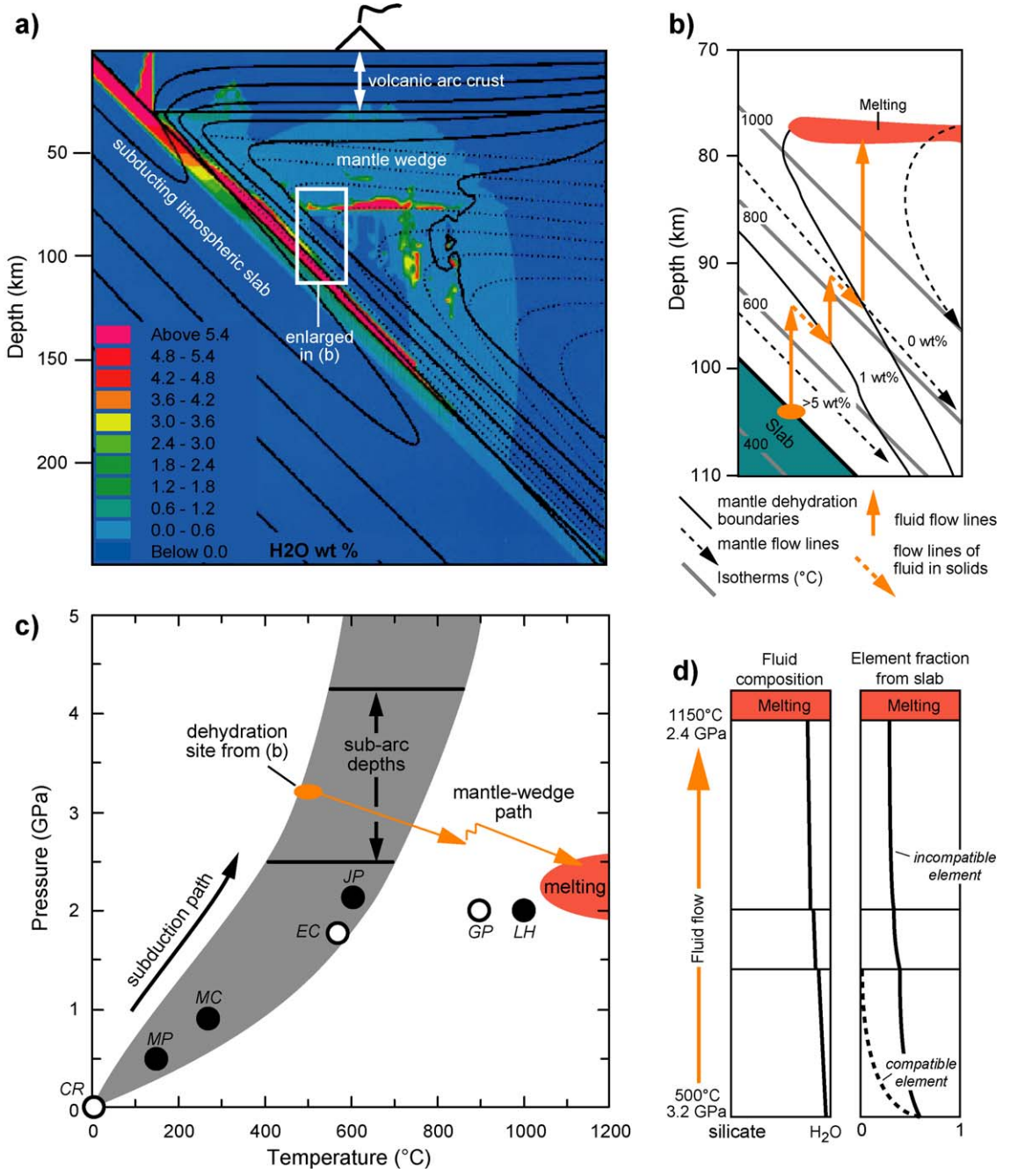

and 1.0–1.1 g/cm^3 at the thermal maximum in the mantle wedge [58–62]. With increasing temperature, the short-range-ordered, tetrahedral packing of H_2O molecules begins to break down. Supercritical H_2O is largely disordered [63,64], and the hydrogen-bond network is disrupted. Although H_2O remains a predominantly molecular solvent up to at least 10 GPa and 1000 °C [65,66], its extent of dissociation increases significantly during subduction (Fig. 2). At sub-arc depths, pure H_2O has between 0.01 and 0.1% H^+ (neutral pH is 3–4). This is significant because, other things being equal, it will raise the concentration of solutes due to an increase in ionic strength.

3.2. Dissociation/association and ion hydration

Pressure and temperature have opposite effects on dissociation of salts in H_2O. At constant P, increasing T causes ions to associate as the dielectric constant of H_2O increases and ion-hydration shells become less stable. At constant T, increasing P causes dissociation by enhancing electrostriction of H_2O around ions, which reduces the volume of solvation. Fig. 2 shows that changes in P and T along subduction paths promote association in dilute solutions; however, dissociation increases dramatically with small increases in concentration. This further increases the capacity to carry dissolved solutes, and magnifies the effects of additional ligands. For example, high Cl in arc lavas [67,68] implies that slab-derived fluids carry chloride. Increasing chlorinity favors solution of metals because of metal-chloride complexing. Calcite and anhydrite solubilities in H_2O–NaCl are dramatically enhanced with increasing NaCl concentration at high pressure [50,69], and

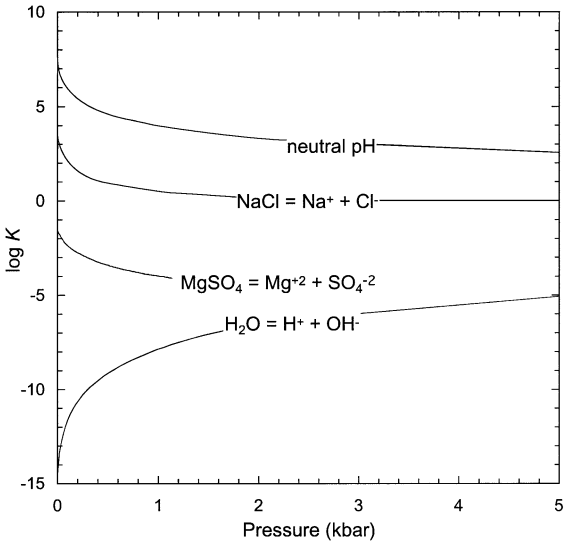

Fig. 2. Extent of dissociation (as measured by equilibrium constant, K) of H_2O, NaCl, and $MgSO_4$ as a function of pressure. H_2O and NaCl dissociation are computed along the high-T part of the envelope of subduction paths in Fig. 1c. See [92] for data sources and methods. $MgSO_4$ is taken from experiments [120] at H_2O density of 1.0 g/cm^3.

Fig. 1. (a) Results of a numerical simulation of H_2O production and migration in a model subduction zone [42]. The model includes solid mantle flow, assumes mineral-fluid-melt equilibrium in the slab (MORB–H_2O) and mantle wedge (peridotite–H_2O) system, and approximates aqueous fluid migration by porous flow along a pressure gradient. Subduction rate is 6 cm/year and the slab is 130 million years old. Colors represent rock H_2O content, solid lines denote isotherms (200 °C intervals, surface is 0 °C), and dashed lines indicate mantle flow paths. The location of the volcanic front is schematic. Water content decreases with depth in the slab due to H_2O loss from hydrous minerals. Large portions of the mantle in the model are at least partly hydrated by this fluid; some fluid crosses the moho and locally reaches the surface. High H_2O contents in the high-T region of the mantle beneath the volcanic arc signify sites where melting can be expected. This conceptual framework is consistent with high-precision studies of trace elements and isotopic variations across and along volcanic arcs [109–118]. (b) Enlargement of region in (a) showing schematic path of a slab-derived fluid, with mantle H_2O contents (wt.%). The fluid migrates into the mantle wedge (solid orange arrows), where it is absorbed through formation of hydrous minerals. Downward flow of solid mantle (dashed arrows) causes dehydration. After multiple hydration–dehydration steps, the fluid enters a region where it is stable with anhydrous minerals, which allows greater travel distances. (c) Pressure–temperature diagram showing representative conditions at the slab–mantle interface (shaded) in northwest and southeast Japan [119], the coolest of which (left side) corresponds to results in (a). The fluid-flow trajectory represents the schematic path from (a) and (b). Also shown are P and T of fluid compositions discussed in the text. Open symbols designate fluids equilibrated with crustal mineral assemblages; filled symbols designate fluids equilibrated with mantle (Table 1). Abbreviations: CR, Costa Rica [83]; MP, Marianas (Pacman Seamount) [82,85]; MC, Marianas (Conical Seamount), [85,108]; EC, MORB eclogite [92]; JP, jadeite peridotite [94]; GP, garnet–orthopyroxene [95]; LH, Lherzolite [96]. (d) Schematic changes in fluid composition along the flow path in (c). Concentration of silicate components derived from the rock matrix increase downstream because of rising temperature, leading to dilution of the slab component. Slab-derived compatible elements are lost close to the slab, but incompatible elements may be transported to the magma source region. In detail patterns will be more complicated owing to changes in mineral stability and fluid flux.

minor-element patterns may be strongly affected [70].

3.3. Critical curves and second critical end points

Interpretation of subduction-zone fluids is made difficult by uncertainty about melt-vapor miscibility and the existence of critical end-points in rock–H_2O systems. It is commonly assumed that fluids in subduction zones may attain properties intermediate between hydrous silicate liquid and H_2O. The expected enhancement of transport has led to the frequent indictment of intermediate fluids as metasomatic agents. However, such fluids exist only under quite restricted conditions, and their direct relevance to subduction zones is problematic. Part of the uncertainty derives from complex relationships whose depiction may seem inscrutable to all but the most ardent fan of phase diagrams. A brief overview is offered here.

3.3.1. Background

One-component systems, such as H_2O or mineral *A* (Fig. 3), possess a critical point marking termination of the distinction between the liquid and the vapor phase. At *T* and *P* above this point, there is only one phase, a supercritical fluid. In a system with both *A* and H_2O, the two critical points are linked together by a "critical curve" that marks the boundary between the stability region of a single supercritical fluid, and that of two fluids, a denser liquid and a less-dense vapor. Another curve extends from the point at which ice and mineral *A* coexist with liquid and vapor (the *A*-ice eutectic). This is the "solubility curve," which marks the stable coexistence of mineral *A* with liquid and vapor (Fig. 3A). Compositions of liquid, gas, and supercritical fluid vary along critical and solubility curves. For example, with increasing *T* along the solubility curve, the liquid composition changes continuously from nearly pure H_2O to pure *A*. At high *T*, where the liquid is rich in *A*, the solubility curve is equivalent to the hydrous melting curve (the "solidus" in the simple system shown). Two-component systems of geologic interest exhibit a range of behaviors. In some, the critical curve and solubility curve remain separated over their entire lengths (Fig. 3A); in others, they intersect (Fig. 3B) to yield two "critical end-points." The lower (first) critical end-point typically lies near the critical point of H_2O. The upper, or second, critical end-point lies at high *P* and *T*, potentially near subduction paths.

3.3.2. Critical behavior in albite–H_2O

The curious relationships indicated by critical behavior, in particular of the second type (Fig. 3B), have led to speculation about a role for supercritical fluids in subduction zones. This can be explored using the system albite–H_2O for illustration. The critical curve of albite–H_2O lies at relatively low *P* (Fig. 4a) [71], below that of melt generation in the mantle wedge. The albite–H_2O critical curve probably intersects the solubility curve at ~ 670 °C, 1.6 GPa (Fig. 4a) [72] to generate a second critical end-point. Two schematic subduction paths illustrate the effects. Along Path 1 (Fig. 4a,b), albite solubility in H_2O increases until, at the solubility curve (H_2O-saturated melting, 685 °C, 1.5 GPa), it is ~ 10 wt.%. Above this point, only hydrous, albite-rich liquid can coexist with H_2O-rich vapor (Fig. 4b). Liquid + vapor become fully miscible at ~ 700 °C, 1.55 GPa (Fig. 4a), which signifies passage of the crest of the liquid + vapor field (Fig. 4b). Along Path 2 (Fig. 4a,c), C2 produces a narrow *PT* region (shaded) in which albite solubility increases continuously in a coexisting fluid that varies from dilute solution to hydrous albite-rich liquid— there is no discrete melting point.

3.3.3. Critical behavior and subduction zones

Despite the intriguing behavior of albite–H_2O, the significance of intermediate fluids in subduction zones is questionable. Critical behavior is strongly dependent on composition. Complete miscibility occurs at low to moderate *P* in many Na-rich systems [73]. Fluorine, boron and excess Na shift the critical curve to dramatically lower *T* at a given *P* [74]. A natural example has been reported in a pegmatite, in which complete miscibility of F-, B- and P-rich fluid occurs at 712 °C, 21.5 wt.% H_2O [75]. However, the critical curves of potassic and mafic systems lie at much higher *P* [76]; e.g., 12 GPa, ~ 1150 °C in $MgO–SiO_2–H_2O$ [77]. The system $K_2O–SiO_2–H_2O$ remains subcritical to at least 2 GPa at 1100 °C [78]. Critical curves for mantle systems (lherzolite–$CO_2–H_2O$) are likely 7.5 GPa or higher at ~ 1000 °C [79]. More information

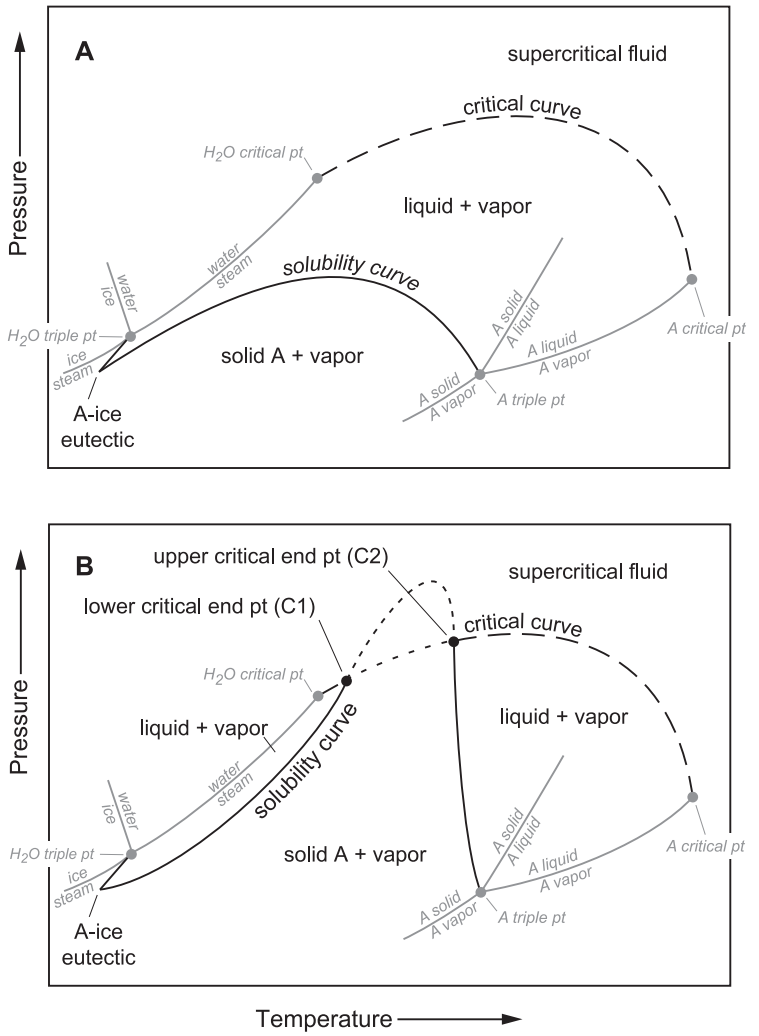

Fig. 3. Schematic $P-T$ projections of phase relations illustrating contrasting behavior of simple two-component systems. Grey lines indicate phase relations for one-component systems H_2O and hypothetical composition A; black lines represent relations for A-H_2O mixtures. Labeling of fields is for H_2O-rich systems. (A) The system A-H_2O, in which the critical curve and solubility curve do not intersect. NaCl–H_2O is an example of such a system. (B) The system A-H_2O, in which the critical curve and solubility curve intersect. This yields two critical end points (C1 and C2). Short dashed lines denote metastable portions of curves. Albite–H_2O is an example.

is needed, but it appears that critical curves for compositions more closely approximating subduction-zone rocks lie at substantially higher P than that for albite–H_2O.

Even if phase relations can be approximated by albite–H_2O, Fig. 4 reveals important restrictions on supercritical fluids. Other phases in the same chemical system may play an important role. Albite transforms to jadeite + quartz at high P, with different solubility and a change in solidus slope (Fig. 4a). No sign of a supercritical fluid has been noted above the solidus at high P, possibly pointing to structural changes in the silicate-rich liquid that could cause the liquid + vapor field to reappear.

Another problem for intermediate fluids is that the critical curve seems to be a feature of very H_2O-rich compositions at the T of interest. Again taking albite–H_2O as a model, a closed system with several wt.%

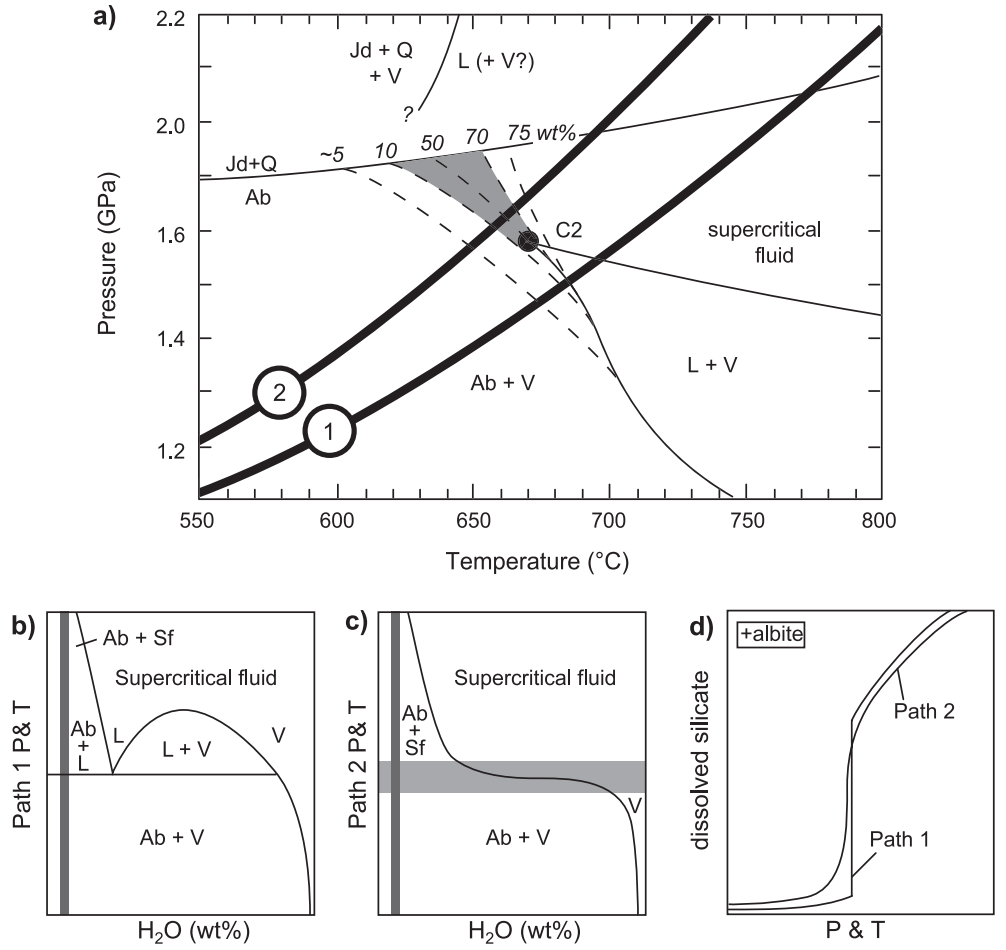

Fig. 4. (a) *PT* diagram illustrating phase relations near the second critical end point (C2) in the system albite–H_2O. Critical curve, solubility curve, and isopleths of albite solubility (dashed, in wt.%) from [71,72]. Thick solid lines represent two schematic subduction paths passing below (1) and above (2) the critical end-point. Shading indicates the region of greatest change in fluid composition. The Jd + Q solidus is queried because it is not known how it is affected by C2. Abbreviations: Ab, albite, Jd, jadeite; L, liquid; Q, quartz; Sf, supercritical fluid; V, vapor. (b) Phase relations of albite–H_2O along Path 1 as function of H_2O concentration. (c) Phase relations of albite–H_2O along Path 2 as a function of H_2O concentration. Light shading represents the region shaded in (a). In (b) and (c), the dark shaded band represents typical H_2O contents of geologic systems. (d) Comparison of the variation in dissolved silicate in the phase coexisting with albite along Paths 1 and 2.

H_2O (Fig. 4b,c) will contain albite everywhere along both paths at conditions in Fig. 4. Such a system on Path 1 will encounter neither the L + V field (which requires more than ~ 20 wt.% H_2O) nor the critical curve (~ 50 wt.% H_2O; Fig. 4b) [71,72]. On Path 2, albite coexists with an intermediate fluid only over a narrow *PT* interval (Fig. 4a,c). Comparison of the compositions of the albite-saturated fluid phase (vapor, liquid, or supercritical fluid; Fig. 4d) shows that little difference results from passage of the critical point. Contrasts between supercritical and subcritical solubility behavior will increase with greater separation of the subduction path from C2, but only if "fanning" of iso-concentration lines increases and there are no other phases (e.g., jadeite and quartz) to change the bulk solubility of the solids (Fig. 4a).

Even if they form, intermediate fluids can only be important metasomatic agents if they separate from their source and travel significant distances. However, with movement comes a new chemical environment

and different P and T. Rocks encountered along the mantle-wedge flow path will not be in equilibrium with the fluid, which will likely result in precipitation of much of the solute load over short length scales.

3.4. Polymerization of silicate components

Although I have argued that fully miscible fluids are not as important in subduction zones as has been supposed, the critical behavior holds a clue to what may be a fundamental aspect of deep fluid chemistry. A supercritical fluid can change continuously from pure H_2O to hydrous melt; i.e., solutes can evolve from hydrated ions or molecules, through small clusters, to the polymerized network of a hydrous silicate liquid. Fully miscible behavior requires that polymerization and network formation by silicate components in the aqueous phase is an important aspect of the chemistry even of dilute H_2O-rich subduction-zone fluids.

An early, direct observation of silicate polymers in dense fluids was by Mysen [78], who identified aqueous silica dimers and trimers coexisting with $K_2O–SiO_2–H_2O$ melts. These structures are marked respectively by two and three Si cations linked by bridging oxygens. Phase-equilibrium and in-situ studies confirm that silica polymerization is significant at subduction-zone P and T [49,52–54]. At 800 °C, 1.2 GPa, aqueous silica is a mix of monomers and dimers, with dimers increasing from 0 to 70% from pure H_2O to quartz saturation [51].

Its predominance in solution and ability to polymerize mean that silica plays a central role in the generation of solute polymers. However, liquid–vapor miscibility in aluminous compositions [71,73] suggests that Al solubility is enhanced because it participates in polymerization, as in silicate liquids. This is consistent with the stability of aqueous Al–Si complexes in crustal fluids [80]. Other elements may have solubility enhanced by participation in aqueous polymerization reactions (e.g., Mg [33,81]). Thus, complexing among Si, Al, and other elements via formation of polymerized solute may play an important role in controlling fluid composition at depth in subduction-zone settings. The partitioning of elements between the bulk fluid, the silicate polymer network in the fluid, and the rock matrix likely controls the overall compositional evolution of subduction-zone fluids. It is possible that concentrations of nominally insoluble elements may be enhanced through their participation in polymers, even in fairly dilute solutions.

4. Composition of subduction-zone fluids

The discussion of physical and chemical controls on subduction-zone fluids provides a framework for examination of constraints on composition. Fig. 1 shows that fluids may be produced over a range in depth, and that their upward flow into the mantle carries them across a major compositional boundary on a path of increasing temperature with decreasing pressure. Fig. 1d illustrates the expected behavior of typical silicate components from the matrix along this path. Solubility will increase because the increase in T has a larger effect than the drop in P. For a slab-derived fluid in the mantle, this leads to dilution of the slab component as the mantle minerals progressively dissolve into the fluid. However, the relative solubility of a given element in the rock vs. the fluid will be a complex function of P, T, and composition. Those elements that are strongly partitioned into the rock relative the fluid (“compatible elements”) will be lost from the fluid very near its source. The result is (1) a metasomatic zone near the slab–mantle interface that is rich in compatible elements such as Si, Ca, Al, etc., and (2) difficulty in transferring the slab signal for such elements far into the mantle. In contrast, elements that are strongly partitioned into the fluid relative to the rock (“incompatible elements”) will remain in the fluid as it travels away from the slab, allowing the compositional signature of the slab to travel well into the mantle wedge. Within this framework, we can examine existing constraints on fluid composition in subduction zones (Table 2).

4.1. Major elements

Direct samples of subduction-zone fluids are available from the Costa Rica and the Izu-Bonin/Mariana convergent margins [82,83]. At Costa Rica, décollement fluids are sourced at 10–15 km, 100–150 °C [84]. They have 28 g/kg H_2O total dissolved solids (TDS), dominated by Na and Cl, with low Si and a modest load of alkali and alkaline earth metals. Chlorinity is below seawater.

Table 2
Comparison of major-element compositions of subduction-zone fluids

	Costa Rica décollement	Marianas (Pacman seamount)	Marianas (Conical seamount)	Model eclogite (~ MORB)	Jadeite peridotite	Garnet + orthopyroxene	Spinel–ilmenite–rutile lherzolite
Depth to slab (km)	0.36	~ 15	~ 25	~ 50			
P (GPa)				1.75	2.2	2.0	2.0
T (°C)				550	600	900	1000
Cl	486	404	315	400		500	
Si	0.084		0.032	356	547	905	285
Al				0.8	99	193	61
Na	411		423	509	121	28	31
K	3.3		15				
Ca	23	47	1.3	8		44	26
Mg	12.9	0	0.005	0.001	3	125	21
Fe						13	11
Ti							3
Alkalinity		1	31				
TDS	28	17	28	48	38	83	67
Source	[83]	[85]	[108]	[92]	[94]	[95]	[96]

Concentrations in millimol per kg H_2O, except alkalinity = meq/kg H_2O, total dissolved solids (TDS) = grams total solute per kg H_2O.

Pore fluids from Mariana forearc serpentine-mud volcanoes originate at the slab–mantle interface at 15–25 km [82,85,86]. Cl concentration is lower than seawater, consistent with a dehydration origin. Ca decreases and CO_2 (alkalinity) increases with depth, reflecting the onset of slab decarbonation between 15- and 25-km depth [85]. Mg and Ca are lower than in Costa Rica fluids, perhaps due to lower chlorinity. Lower Si probably reflects the serpentinite host.

Direct samples have unknown reaction-flow history prior to sampling, so conditions of last equilibration are unclear. Fluid inclusions in exhumed blueschist- and eclogite-facies oceanic mafic rocks represent an alternative sample. Fluids show 1–7 wt.% NaCl equivalent [87], or TDS = 10–75 g/kg H_2O. This spans values of shallow fluids. Increases in TDS with depth over 25–50 km are no more than about a factor of two, and low salinity and CO_2 indicate that H_2O is the dominant solvent.

It is important to note that primary fluid inclusions in eclogites associated with continental subduction may have much higher N_2, CO_2, and salinity (up to 50 wt.% NaCl equivalent) [11,88–91]. There appears to be a fundamental difference in the salinity of fluids associated with oceanic and continental subduction, as recorded by fluid inclusions. Cross-comparisons between fluids in these two environments require extreme caution.

In the absence of direct samples of unreacted fluids or fluid inclusions, we must rely on estimates from mineralogic phase relations and experiments. Theoretical analysis of deeper fluid produced at the blueschist-eclogite transition indicates yet higher TDS (48 g/kg H_2O) [92]. This is largely due to the dramatic increase in silica at similar Cl content. Na and Ca concentrations are broadly similar. Al concentration, which is so low in low-pressure fluids that it is rarely analyzed, is higher than Mg. Varying Cl does not have a large effect. The high Al suggests that deep fluids leaving the slab are Na–Ca–Al–Si rich, but low in Mg and Fe, unless significant Cl is present. This is consistent with vein minerals in blueschists and eclogites [87,93].

Insights into the compositional evolution of slab-derived fluids as they react with the mantle wedge can be gained from experimental studies. Aqueous fluid in equilibrium with jadeite–peridotite at conditions near the slab–mantle interface (Fig. 1) is Si- and Na-rich, and contains substantial Al [94]. Total dissolved solids is similar to the results for eclogite with Cl-free fluid. The higher Si reflects the strong dependence of Si concentration on temperature at high pressure [49].

In the region of arc-magma generation, a 5-molal NaCl solution in equilibrium with garnet and orthopyroxene at 900 °C, 2 GPa, has nearly twice the silica, as well as higher Mg, Ca, and Al, low Na and

Fe, TDS of 83 g/kg H_2O [95]. H_2O equilibrated with spinel lherzolite and Ti phases at 2.0 GPa, 1000 °C, shows lower Na, Al, and Si, but is otherwise similar to the garnet–orthopyroxene fluid [96]. Differences in Na between the fluids at 900–1000 °C and those at 550–660 °C are probably due to varying Na in the buffering assemblage.

Three important conclusions can be drawn from Table 2 about the major-element compositions of subduction-zone fluids. First, the deeper fluids are similar to the direct, shallow samples in one important way: total solute concentrations are low, regardless of pressure, temperature, or chlorinity. Deep fluids have TDS only two to three times that of seawater, and no more than 50% higher than shallow fluids from near the entrance to the subduction zone. TDS does not approach tens of wt.%, as would be associated with supercritical fluids of intermediate composition (Fig. 4). This is consistent with the independent arguments developed above.

The second conclusion is that TDS, though generally modest, nevertheless increases with depth. This arises from changes in solubility of rock-forming minerals due to the *PT*-enhancement of the solvent power of H_2O; additional ligands such as Cl may be present, but are not required.

Finally, there are important changes in major elements with depth. The dominant solutes in deep fluids are Si and Na. Al concentrations are higher than Ca, Fe, and usually Mg. Thus, the solutes in H_2O-rich fluids in subduction zones are dominated by alkali and aluminosilicate components. This contrasts with fluids from shallow environments, where alkali and other metals predominate and Al is virtually insoluble. It is quite likely that this change with increasing depth in subduction zones simply reflects the ability of alkali aluminosilicate components to form aqueous polymers at high *P* and *T*.

4.2. Trace elements

Trace-element patterns support the inference that the continental crust formed by island-arc magmatism (Fig. 5), but enrichments and depletions preclude simple anhydrous melting and fractionation. Instead, arc-magmas form by hydrous melting of a source metasomatized by slab-derived components. Trace-element patterns of low-Cl subduction-zone

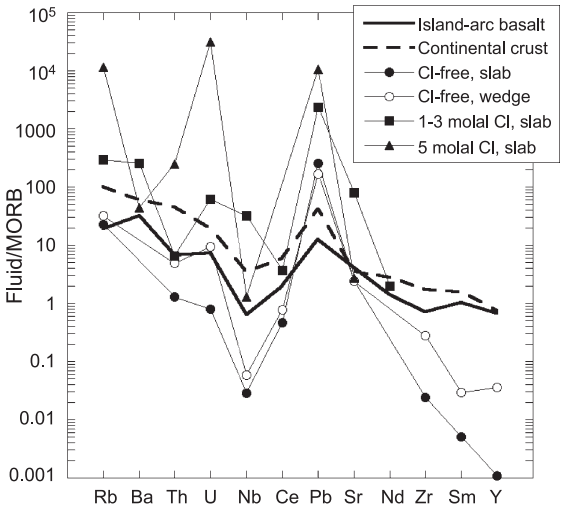

Fig. 5. Trace-element diagram normalized to MORB [121]. Elements are plotted in order of decreasing compatibility from left to right. Trace-element patterns grouped by chlorine concentration: Cl-free [97]; 1–3 molal [89]; 5 molal [70]. Island-arc basalt from [122]; continental crust from [123].

fluids are broadly similar to island-arc basalt (IAB) and continental crust, with enrichments in LILE and Pb, and depletions in high field strength elements (Fig. 5). However, >1 molal chloride changes some aspects of the patterns [70]. While Pb enrichment, Nb depletion, and a decreasing abundance with compatibility remain, the 5 molal brine shows very high Rb/Ba, Th/U ~ 0.01, enhanced Pb enrichment, and extreme differences between adjacent elements. This would appear to suggest that the trace-element signature of the IAB source is controlled by flow of low-Cl fluid [97,98]. However, the simple model compositions require more H_2O in the IAB source than is typically inferred [12], and isotopic studies support a wide range of chlorinity [99–102]. While there are likely to be real variations in Cl content in the global subduction system, there is also a need for more sophisticated reactive flow models that account for changes in mantle mineral assemblage along with evolution of fluid and rock composition.

5. Prospects for the future

This paper has attempted to highlight some of the open questions regarding the chemistry of

subduction-zone fluids. H_2O is a powerful solvent at subduction zone conditions, and it can effectively mobilize many rock components. Although supercritical, intermediate fluids are commonly invoked to explain mantle-wedge metasomatism, the hypothesis is problematic in detail. Supporting this, theoretical and experimental constraints on fluids at sub-arc conditions are surprisingly dilute. It may be that the chemistry of aqueous silicate polymers, as controlled by *P*, *T* and the mineralogy of the host, plays a fundamental role in the composition of subduction-zone fluids. The effects of Cl, and by inference other ligands, may be profound, but it is unclear at this time what role is required of them.

There are excellent prospects for progress on these issues in the near future. Experimental advances, including the hydrothermal diamond anvil cell [103–106] and solid media solubility techniques [48–51], promise to provide fundamental data on mineral solubility and fluid composition. Advances in molecular dynamics and ab-initio molecular dynamics simulations are already giving unprecedented insight into the nature of H_2O and ion hydration, geometry and structure [64,107]. Finally, new geochemical tools, including light element isotope ratios (e.g., Li and B), new spectroscopic methods and ICP-MS, are being applied to fluid and melt inclusions in subducted oceanic rocks, mantle-wedge xenoliths and arc magmas. Results give new insight into the details of slabs and arc-magma sources, which constrain the initial and final conditions in the reacting system of interest here.

The new data will provide the foundation necessary to develop sophisticated reaction-flow models of this complex metasomatic environment. Once this is under way, we will have made a major advance toward unraveling the chemical workings of this part of the subduction factory.

Acknowledgements

This study was supported by NSF EAR 9909583 and 0337170. Reviews by J. Ayers, G. Bebout and an anonymous reviewer improved the manuscript. I am also indebted to R. Newton, J. Davidson, and S. Peacock for insightful critiques. ***[AH]***

References

[1] G.E. Bebout, J.G. Ryan, W.P. Leeman, A.E. Bebout, Fractionation of trace elements by subduction zone metamorphism—effect of convergent margin thermal evolution, Earth Planet. Sci. Lett. 171 (1999) 63–82.

[2] D.R. Hilton, T.P. Fischer, B. Marty, Noble gases and volatile recycling at subduction zones, Rev. Mineral. Geochem. 47 (2002) 319–370.

[3] R.D. Jarrard, Subduction fluxes of water, CO_2, chlorine, and potassium, Geochim. Geophys. Geosys. 4 (2003) DOI:10.1029/2002GC000392.

[4] S.J. Sadofsky, G.E. Bebout, Record of forearc devolatilization in low-*T*, high *P*/*T* metasedimentary suites: significance for models of convergent margin chemical cycling, Geochem. Geophys. Geosys. 4 (4) (2003) 29 pp.

[5] J.M. Eiler, B. McInnes, J.W. Valley, C.M. Graham, E.M. Stolper, Oxygen isotope evidence for slab-derived fluids in the sub-arc mantle, Nature 393 (1998) 777–781.

[6] J.M. Eiler, A. Crawford, T. Elliott, K.A. Farley, J.W. Valley, E.M. Stolper, Oxygen isotope geochemistry of oceanic-arc lavas, J. Petrol. 41 (2000) 229–256.

[7] I.J. Parkinson, R.J. Arculus, The redox state of subduction zones: insights from arc-peridotites, Chem. Geol. 160 (1999) 409–424.

[8] R.J. Stern, Subduction zones, Rev. Geophys. 40 (4) (2002) 3-1–3-38.

[9] P.E. van Keken, The structure and dynamics of the mantle wedge, Earth Planet. Sci. Lett. 215 (2003) 323–338.

[10] B.O. Mysen, P. Ulmer, J. Konzett, M.W. Schmidt, The upper mantle near convergent plate boundaries, Rev. Mineral. 37 (1998) 97–138.

[11] M. Scambelluri, P. Phillipot, Deep fluids in subduction zones, Lithos 55 (2001) 213–227.

[12] P. Ulmer, Partial melting in the mantle wedge—the role of H_2O in the genesis of mantle-derived "arc-related" magmas, Phys. Earth Planet. Inter. 127 (2001) 215–232.

[13] S. Poli, M.W. Schmidt, Petrology of subducted slabs, Ann. Rev. Earth Planet. Sci. 30 (2002) 207–335.

[14] P.S. Hall, C. Kincaid, Diapiric flow at subduction zones: a recipe for rapid transport, Science 292 (2001) 2472–2475.

[15] J.F. Molina, S. Poli, Carbonate stability and fluid composition in subducted oceanic crust: an experimental study on H_2O-CO_2-bearing basalts, Earth Planet. Sci. Lett. 176 (2000) 295–310.

[16] D.M. Kerrick, J.A.D. Connolly, Metamorphic devolatilization of subducted oceanic metabasalts: implications for seismicity, arc magmatism and volatile recycling, Earth Planet. Sci. Lett. 189 (2001) 19–29.

[17] D.M. Kerrick, J.A.D. Connolly, Metamorphic devolatilization of subducted marine sediments and the transport of volatiles into the Earth's mantle, Nature 411 (2001) 293–296.

[18] S.M. Peacock, Are the lower planes of double seismic zones caused by serpentine dehydration in subducting oceanic mantle? Geology 29 (2001) 299–302.

[19] B.R. Hacker, G.A. Abers, S.M. Peacock, Subduction factory: 1. Theoretical mineralogy, density, seismic wave speeds, and

H_2O content, J. Geophys. Res. 108 (2003) DOI:10.1029/2001JB001127.
[20] B.R. Hacker, S.M. Peacock, G.A. Abers, S.D. Holloway, Subduction factory: 2. Are intermediate-depth earthquakes in subducting slabs linked to metamorphic dehydration reactions? J. Geophys. Res. 108 (2003) DOI:10.1029/2001JB001129.
[21] M.W. Schmidt, S. Poli, Experimentally based water budgets for dehydrating slabs and consequences for arc magma generation, Earth Planet. Sci. Lett. 163 (1998) 361–379.
[22] T. Moriguti, E. Nakamura, Across-arc variation of Li isotopes in lavas and implications for crust/mantle recycling at subduction zones, Earth Planet. Sci. Lett. 163 (1998) 167–174.
[23] S. Peacock, R.L. Hervig, Boron isotopic composition of subduction-zone metamorphic rocks, Chem. Geol. 160 (1999) 281–290.
[24] S.M. Straub, G.D. Layne, The systematics of boron isotopes in Izu arc front volcanic rocks, Earth Planet. Sci. Lett. 198 (2002) 25–39.
[25] P.E. van Keken, B. Kiefer, S.M. Peacock, High-resolution models of subduction zones: implications for mineral dehydration reactions and the transport of water into the deep mantle, Geochim. Geophys. Geosys. 3 (2002) DOI: 10.1029/2001GC000256.
[26] P.B. Tomascak, E. Widom, L.D. Benton, S.L. Goldstein, J.G. Ryan, The control of lithium budgets in island arcs, Earth Planet. Sci. Lett. 196 (2002) 227–238.
[27] G.E. Bebout, E. Nakamura, Record in metamorphic tourmalines of subduction-zone devolatilization and boron cycling, Geology 31 (2003) 407–410.
[28] T. Zack, P.B. Tomascak, R.L. Rudnick, C. Dalpé, W.F. McDonough, Extremely light Li in orogenic eclogites: the role of isotope fractionation during dehydration in subducted oceanic crust, Earth Planet. Sci. Lett. 208 (2003) 279–290.
[29] K. Obara, Nonvolcanic deep tremor associated with subduction in southwest Japan, Science 296 (2002) 1679–1681.
[30] B. Wunder, Equilibrium experiments in the system $MgO–SiO_2–H_2O$ (MSH): stability fields of clinohumite–OH $[Mg_9Si_4O_{16}(OH)_2]$, chondrodite $[Mg_5Si_2O_8(OH)_2]$ and phase A $[Mg_7Si_2O_8(OH)_6]$, Contrib. Mineral. Petrol. 132 (1998) 111–120.
[31] A. Pawley, Stability of clinohumite in the system $MgO–SiO_2–H_2O$, Contrib. Mineral. Petrol. 138 (2000) 284–291.
[32] A. Pawley, Chlorite stability in mantle peridotite: the reaction clinochlore plus enstatite = forsterite + pyrope + H_2O, Contrib. Mineral. Petrol. 144 (2003) 449–456.
[33] R. Stalder, P. Ulmer, Phase relations of a serpentine composition between 5 and 14 GPa: significance of clinohumite and phase E as water carriers into the transition zone, Contrib. Mineral. Petrol. 140 (2001) 670–679.
[34] Q. Williams, R.J. Hemley, Hydrogen in the deep earth, Annu. Rev. Earth Planet Sci. 29 (2001) 365–418.
[35] G.D. Bromiley, A.R. Pawley, The high-pressure stability of Mg-surassite in a model hydrous peridotite: a possible mechanism for the deep subduction of significant volumes of H_2O, Contrib. Mineral. Petrol. 142 (2002) 714–723.
[36] K. Litasov, E. Ohtani, Stability of various hydrous phases in CMAS pyrolite–H_2O system up to 25 GPa, Phys. Chem. Miner. 30 (2003) 147–156.
[37] J.F. Forneris, J.R. Holloway, Phase equilibria in subducting basaltic crust: implications for H_2O release from the slab, Earth Planet. Sci. Lett. 214 (2003) 187–201.
[38] I. Cartwright, A.C. Barnicoat, Stable isotope geochemistry of Alpine ophiolites: a window to ocean-floor hydrothermal alteration and constraints on fluid–rock interaction during high-pressure metamorphism, Int. J. Earth Sci. 88 (1999) 219–235.
[39] S.M. Peacock, R.D. Hyndman, Hydrous minerals in the mantle wedge and the maximum depth of subduction thrust earthquakes, Geophys. Res. Lett. 26 (1999) 2517–2520.
[40] M.G. Bostock, R.D. Hyndman, S. Rondenay, S.M. Peacock, An inverted continental Moho and serpentinization of the forearc mantle, Nature 417 (2002) 536–538.
[41] T. Mastsumoto, T. Kawabata, J.-I. Matsuda, K. Yamamoto, K. Mimura, $^3He/^4He$ ratios in well gases in the Kinki district, SW Japan: surface appearance of slab-derived fluids in a non-volcanic area, Earth Planet. Sci. Lett. 216 (2003) 221–230.
[42] H. Iwamori, Transportation of H_2O and melting in subduction zones, Earth Planet. Sci. Let. 160 (1998) 65–80.
[43] K. Mibe, T. Fujii, A. Yasuda, Control of the location of the volcanic front in island arcs by aqueous fluid connectivity in the mantle wedge, Nature 401 (1999) 259–262.
[44] G.H. Davies, The role of hydraulic fractures and intermediate-depth earthquakes in generating subduction-zone magmatism, Nature 398 (1999) 142–145.
[45] D.P. Dobson, P.G. Meredith, S.A. Boon, Simulation of subduction zone seismicity by dehydration of serpentine, Science 298 (2002) 1407–1410.
[46] S.P. Turner, On the time-scales of magmatism at island-arc volcanoes, Philos. Trans. R. Soc. Lond. Ser. A: Math. Phys. Sci. 360 (2002) 2853–2871.
[47] T. Yokoyama, E. Nakamura, K. Kobayashi, T. Kuritani, Timing and trigger of arc volcanism controlled by fluid flushing from subducting slab, Proc. Jpn. Acad., Ser. B Phys. Biol. Sci. 78 (2002) 190–195.
[48] R.C. Newton, C.E. Manning, Quartz solubility in concentrated aqueous NaCl solutions at deep crust–upper mantle metamorphic conditions: 2–15 kbar and 500–900 °C, Geochim. Cosmochim. Acta 64 (2000) 2993–3005.
[49] R.C. Newton, C.E. Manning, Solubility of enstatite + forsterite in H_2O at deep crust/upper mantle conditions: 4 to 15 kbar and 700 to 900 °C, Geochim. Cosmochim. Acta 66 (2002) 4165–4176.
[50] R.C. Newton, C.E. Manning, Experimental determination of calcite solubility in $H_2O–NaCl$ solutions at deep crust/upper mantle pressures and temperatures: implications for metasomatic processes in shear zones, Am. Mineral. 87 (2002) 1401–1409.
[51] R.C. Newton, C.E. Manning, Activity coefficient and polymerization of aqueous silica at 800 °C, 12 kbar, from solubility measurements on SiO_2-buffering mineral assemblages, Contrib. Mineral. Petrol. 146 (2003) 135–143.

[52] Y.G. Zhang, J.D. Frantz, Enstatite–forsterite–water equilibria at elevated temperatures and pressures, Am. Mineral. 85 (2000) 918–925.
[53] N. Zotov, H. Keppler, In-situ Raman spectra of dissolved silica species in aqueous fluids to 900 °C and 14 kbar, Am. Mineral. 85 (2000) 600–603.
[54] N. Zotov, H. Keppler, Silica speciation in aqueous fluids at high pressures and high temperatures, Chem. Geol. 184 (2002) 71–82.
[55] K. Shmulovich, C. Graham, B. Yardley, Quartz, albite and diopside solubilities in H_2O–NaCl and H_2O–CO_2 fluids at 0.5–0.9 GPa, Contrib. Mineral. Petrol. 141 (2001) 95–108.
[56] T. Fockenberg, M. Burchard, W.V. Maresch, Experimental determination of the solubility of natural wollastonite in pure water up to pressures of 5.0 GPa, Eos Trans. AGU 83 (47) (2002) (Fall Meet. Suppl. Abstract V72–1327).
[57] N. Caciagli, C.E. Manning, The solubility of calcite in water at 6–16 kbar and 500–800 °C, Contrib. Mineral. Petrol. 146 (2003) 275–285.
[58] S. Wiryana, L.J. Slutsky, J.M. Brown, The equation of state of water to 200 °C and 3.5 GPa: model potentials and the experimental pressure scale, Earth Planet. Sci. Lett. 163 (1998) 123–130.
[59] A.C. Withers, S.C. Kohn, R.A. Brooker, B.J. Wood, A new method for determining the P–V–T properties of high-density H_2O using NMR: results at 1.4–4.0 GPa and 700–1100 °C, Geochim. Cosmochim. Acta 64 (2000) 1051–1057.
[60] W. Wagner, A. Pruss, The IAPWS formulation (1995) for the thermodynamic properties of ordinary water substance for general and scientific use, J. Phys. Chem. Ref. Data 31 (2002) 387–535.
[61] S.V. Churakov, M. Gottschalk, Perturbation theory based equation of state for polar molecular fluid: I. Pure fluids, Geochim. Cosmochim. Acta 67 (2003) 2397–2414.
[62] E.H. Abrahmson, J.M. Brown, Equation of state of water based on speeds of sound measured in the diamond-anvil cell, Geochim. Cosmochim. Acta 68 (2004) 1827–1835.
[63] A.K. Soper, The radial distribution functions of water and ice from 220 to 673 K and at pressures up to 400 MPa, Chem. Phys. 258 (2000) 121–137.
[64] A.G. Kalinichev, Molecular simulations of liquid and supercritical water: thermodynamics, structure, hydrogen bonding, Rev. Mineral. Geochem. 42 (2001) 83–129.
[65] G.A. Lyzenga, T.J. Ahrens, W.J. Nellis, A.C. Mitchell, The temperature of shock-compressed water, J. Chem. Phys. 76 (1982) 6282–6286.
[66] R. Chau, A.C. Mitchell, R.W. Minich, W.J. Nellis, Electrical conductivity of water compressed dynamically to pressures of 70–180 GPa (0.7–1.8 Mbar), J. Chem. Phys. 114 (2001) 1361–1365.
[67] J.D. Webster, R.J. Kinzler, E.A. Mathez, Chloride and water solubility in basalt and andesite melts and implications for magmatic degassing, Geochim. Cosmochim. Acta 63 (1999) 729–738.
[68] A.J.R. Kent, D.W. Peate, S. Newman, E.M. Stolper, J.A. Pearce, Chlorine in submarine glasses from the Lau Basin: seawater contamination and constraints on the composition of slab-derived fluids, Earth Planet. Sci. Lett. 202 (2002) 361–377.
[69] R.C. Newton, C.E. Manning, Stability of anhydrite, $CaSO_4$, in NaCl–H_2O solutions at high pressures and temperatures: applications to fluid–rock interaction, J. Petrol. (in press).
[70] H. Keppler, Constraints from partitioning experiments on the composition of subduction-zone fluids, Nature 380 (1996) 237–240.
[71] A. Shen, H. Keppler, Direct observation of complete miscibility in the albite–H_2O system, Nature 385 (1997) 710–712.
[72] R. Stalder, P. Ulmer, A.B. Thompson, D. Günther, Experimental approach to constrain second critical end points in fluid/silicate systems: near-solidus fluids and melts in the system albite–H_2O, Am. Mineral. 85 (2000) 68–77.
[73] H. Bureau, H. Keppler, Complete miscibility between silicate melts and hydrous fluids in the upper mantle: experimental evidence and geochemical implications, Earth Planet. Sci. Lett. 165 (1999) 187–196.
[74] J.R. Sowerby, H. Keppler, The effect of fluorine, boron and excess sodium on the critical curve in the albite–H_2O system, Contrib. Mineral. Petrol. 143 (2002) 32–37.
[75] R. Thomas, J.D. Webster, W. Heinrich, Melt inclusions in pegmatite quartz: complete miscibility between silicate melts and hydrous fluids at low pressure, Contrib. Mineral. Petrol. 139 (2000) 394–401.
[76] B.O. Mysen, Solubility behavior of alkaline earth and alkali aluminosilicate components in aqueous fluids in the earth's upper mantle, Geochim. Cosmochim. Acta 66 (2002) 2421–2438.
[77] R. Stalder, P. Ulmer, A.B. Thompson, D. Günther, High pressure fluids in the system MgO–SiO_2–H_2O under upper mantle conditions, Contrib. Mineral. Petrol. 140 (2001) 607–618.
[78] B.O. Mysen, Interaction between aqueous fluid and silicate melt in the pressure and temperature regime of the earth's crust and upper mantle, N. Jb. Miner. Ab. 172 (1998) 227–244.
[79] P.J. Wyllie, I.D. Ryabchikov, Volatile components, magmas, and critical fluids in upwelling mantle, J. Petrol. 41 (2000) 1195–1206.
[80] S. Salvi, G.S. Pokrovski, J. Schott, Experimental investigation of aluminum–silica aqueous complexing at 300 °C, Chem. Geol. 151 (1998) 51–67.
[81] K. Mibe, T. Fujii, A. Yasuda, Composition of aqueous fluid coexisting with mantle minerals at high pressure and its bearing on the differentiation of the earth's mantle, Geochim. Cosmochim. Acta 66 (2002) 2273–2285.
[82] P. Fryer, J.A. Pearce, L.B. Stokking, et al, Proc. ODP, Init. Rept., 125, 1990, 1092 pp.
[83] G. Kimura, E. Silver, P. Blum, et al, Proc. ODP, Init. Rept., 170, 1997, 458 pp.
[84] E. Silver, M. Kastner, A. Fisher, J. Morris, K. McIntosh, D. Saffer, Fluid flow paths in the middle America Trench and Costa Rica margin, Geology 28 (2000) 679–682.
[85] P. Fryer, C.G. Wheat, M.J. Mottl, Mariana blueschist mud volcanism: implications for conditions within the subduction zone, Geology 27 (1999) 103–106.

[86] L.D. Benton, J.G. Ryan, F. Tera, Boron isotope systematics of slab fluids as inferred from a serpentine seamount, Mariana forearc, Earth Planet. Sci. Lett. 187 (2001) 273–282.
[87] J. Gao, R. Klemd, Primary fluids entrapped at blueschist to eclogite transition: evidence from the Tianshan meta-subduction complex in northwest China, Contrib. Mineral. Petrol. 142 (2001) 1–14.
[88] M. Scambelluri, P. Philippot, G. Pennacchioni, Salt-rich aqueous fluids formed during eclogitization of metabasites in the Alpine continental crust (Austroalpine Mt. Emilius unit, Italian western Alps), Lithos 43 (1998) 151–161.
[89] M. Scambelluri, P. Bottazzi, V. Trommsdorff, R. Vannucci, J. Hermann, M.T. Gòmez-Pugnaire, V. Lòpez-Sànchez Vizcaìno, Incompatible element-rich fluids released by antigorite breakdown in deeply subducted mantle, Earth Planet. Sci. Lett. 192 (2002) 457–470.
[90] B. Fu, J.L.R. Touret, Y.F. Zheng, Fluid inclusions in coesite-bearing eclogites and jadeite quartzite at Shuanghe, Dabie Shan (China), J. Metamorph. Geol. 19 (2001) 531–547.
[91] L. Franz, R.L. Romer, R. Klemd, R. Schmid, R. Oberhänsli, T. Wagner, S.W. Dong, Eclogite-facies quartz veins within metabasites fo the Dabie Shan (eastern China): pressure–temperature–time–deformation path, composition of the fluid phase and fluid flow during exhumation of high-pressure rocks, Contrib. Mineral. Petrol. 141 (2001) 322–346.
[92] C.E. Manning, Fluid composition at the blueschist–eclogite transition in the model system Na_2O–MgO–Al_2O_3–SiO_2–H_2O–HCl, Swiss Bull. Mineral. Petrol. 78 (1998) 225–242.
[93] H. Becker, K.P. Jochum, R.W. Carlson, Constraints from high-pressure veins in eclogites on the composition of hydrous fluids in subduction zones, Chem. Geol. 160 (1999) 291–308.
[94] M.E. Schneider, D.H. Eggler, Fluids in equilibrium with peridotite minerals: implications for mantle metasomatism, Geochim. Cosmochim. Acta 50 (1986) 711–724.
[95] J.M. Brenan, H.F. Shaw, F.J. Ryerson, Experimental evidence for the origin of lead enrichment in convergent-margin magmas, Nature 378 (1995) 54–56.
[96] J. Ayers, S.K. Dittmer, G.D. Layne, Partitioning of elements between peridotite and H_2O at 2.0–3.0 GPa and 900–1100 °C, and application to models of subduction zone processes, Earth Planet. Sci. Lett. 150 (1997) 381–398.
[97] J. Ayers, Trace element modeling of aqueous fluid–peridotite interaction in the mantle wedge of subduction zones, Contrib. Mineral. Petrol. 132 (1998) 390–404.
[98] R. Stalder, S.F. Foley, G.P. Brey, I. Horn, Mineral-aqueous fluid partitioning of trace elements at 900–1200 °C and 3.0–5.7 GPa: new experimental data for garnet, clinopyroxene, and rutile, and implications for mantle metasomatism, Geochim. Cosmochim. Acta 62 (1998) 1781–1801.
[99] K. Righter, J.T. Chesley, J. Ruiz, Genesis of primitive, arc-type basalt: constraints from Re, Os, and Cl on the depth of melting and role of fluids, Geology 20 (2002) 619–622.
[100] A. Laurora, M. Mazzucchelli, G. Rivalenti, R. Vannucci, A. Zanetti, M.A. Barbieri, A. Cingolani, Metasomatism and melting in carbonated peridotite xenoliths from the mantle wedge: the Gobernador Gregores case (southern Patagonia), J. Petrol. 42 (2001) 69–87.
[101] E. Widom, P. Kepezhinskas, M. Defant, The nature of metasomatism in the sub-arc mantle wedge: evidence from Re–Os isotopes in Kamchatka peridotite xenoliths, Chem. Geol. 196 (2003) 283–306.
[102] P. Kepezhinskas, M.J. Defant, E. Widom, Abundance and distribution of PGE and Au in the island-arc mantle: implications for sub-arc metasomatism, Lithos 60 (2002) 113–128.
[103] W.A. Bassett, A.J. Anderson, R.A. Mayanovic, I.M. Chou, Modified hydrothermal diamond anvil cells for XAFS analyses of elements with low energy absorption edges in aqueous solutions at sub- and supercritical conditions, Zeit. Kristallog. 215 (2000) 711–717.
[104] C. Schmidt, M.A. Ziemann, In-situ Raman spectroscopy of quartz: a pressure sensor for hydrothermal diamond-anvil cell experiments at elevated temperatures, Am. Mineral. 85 (2000) 1725–1734.
[105] C. Schmidt, K. Rickers, In-situ determination of mineral solubilities in fluids using a hydrothermal diamond-anvil cell and SR-XRF: solubility of AgCl in water, Am. Mineral. 88 (2003) 288–292.
[106] M. Burchard, A.M. Zaitsev, W.V. Maresch, Extending the pressure and temperature limits of hydrothermal diamond anvil cells, Rev. Sci. Instrum. 74 (2003) 1263–1266.
[107] D.M. Sherman, Quantum chemistry and classical simulations of metal complexing in aqueous solutions, Rev. Mineral. Geochem. 42 (2001) 273–317.
[108] M.J. Mottl, Pore waters from serpentinite seamounts in the Mariana and Izu-Bonin forearcs, Leg 125 (1992) 373–385.
[109] J.D. Woodhead, S.M. Eggins, R.W. Johnson, Magma genesis in the New Britain Island Arc: further insights into melting and mass transfer processes, J. Petrol. 39 (1998) 1641–1668.
[110] T. Ishikawa, F. Tera, Two isotopically distinct fluid components involved in the Mariana arc: evidence from Nb/B ratios and B, Sr, Nd, and Pb isotope systematics, Geology 27 (1999) 83–86.
[111] C. Class, D.M. Miller, et al, Distinguishing melt and fluid subduction components in Umnak Volcanics, Aleutian Arc, Geochem. Geophys. Geosys. 1 (2000) DOI:10.1029/1999GC000010.
[112] P.W. Reiners, P.E. Hammond, J.M. McKenna, R.A. Duncan, Young basalts of the central Washington Cascades, flux melting of the mantle, and trace element signatures of primary arc magmas, Contrib. Mineral. Petrol. 138 (2000) 249–264.
[113] A. Hochstaedter, J. Gill, R. Peters, P. Broughton, P. Holden, B. Taylor, Across-arc geochemical trends in the Izu-Bonin arc: contributions from the subducting slab, Geochim. Geophys. Geosys. 2 (2001) DOI:10.1029/2000GC000105.
[114] T. Ishikawa, F. Tera, T. Nakazawa, Boron isotope and trace element systematics of the three volcanic zones in the Kamchatka arc, Geochim. Cosmochim. Acta 65 (2001) 4523–4537.
[115] T. Churikova, F. Dorendorf, G. Wörner, Sources and fluids in the mantle wedge below Kamchatka, evidence from across-arc geochemical variation, J. Petrol. 42 (2001) 1567–1593.

[116] M.A. Elburg, M. van Bergen, J. Hoogewerff, J. Foden, P. Vroon, I. Zulkarnain, A. Nasution, Geochemical trends across an arc-continent collision zone: magma sources and slab-wedge transfer processes below the Pantar Strait volcanoes, Indonesia, Geochim. Cosmochim. Acta 66 (2002) 2771–2789.

[117] P. Cervantes, P.J. Wallace, The role of H_2O in subduction zone magmatism: new insights from melt inclusions in high-Mg basalts from Central Mexico, Geology 31 (2003) 235–238.

[118] O. Ishizuka, R.N. Taylor, J.A. Milton, R.W. Nesbitt, Fluid–mantle interaction in an intra-oceanic arc: constraints from high-precision Pb isotopes, Earth Planet. Sci. Lett. 211 (2003) 221–236.

[119] S.M. Peacock, K. Wang, Seismic consequences of warm versus cool subduction metamorphism: examples from southwest and northeast Japan, Science 286 (1999) 937–939.

[120] J.D. Frantz, J. Dubessy, B.O. Mysen, Ion-pairing in aqueous $MgSO_4$ solutions along an isochore to 500 °C and 11 kbar using Raman spectroscopy in conjunction with the diamond-anvil cell, Chem. Geol. 116 (1994) 181–188.

[121] S.-S. Sun, W.F. McDonough, Chemical and isotopic systematics of oceanic basalts: implications for mantle composition and processes, in: A.D. Saunders, M.J. Norry (Eds.), Magmatism in the Ocean Basins, Geol. Soc. London Spec. Publ., vol. 42, (1989) 313–345.

[122] M.T. McCulloch, J.A. Gamble, Geochemical and geodynamical constraints on subduction zone magmatism, Earth Planet. Sci. Lett. 102 (1991) 358–374.

[123] B.S. Kamber, A. Ewart, K.D. Collerson, M.C. Bruce, G.D. MacDonald, Fluid-mobile trace element constraints on the role of slab melting and implications for Archaean crustal growth models, Contrib. Mineral. Petrol. 144 (2002) 38–56.

Craig Manning is a Professor of Geology and Geochemistry in the Department of Earth and Space Sciences at the University of California Los Angeles. He received BA degrees in Geology and in Geography from the University of Vermont, and MS and PhD degrees in Geology from Stanford University. His current research focuses on experimental and theoretical study of mineral solubility in geologic fluids at high pressure and temperature, the role of subduction-zone fluids in geochemical cycles, Archean hydrothermal systems, and the geology and tectonics of central Asia.